

A Numerical study on the effect of solid boundaries on the density-driven laminar flows

Himanshu Kishnani¹, Abhishek Kundu¹

¹Applied Mechanics Department, MNNIT Allahabad, Prayagraj-211004, India

ABSTRACT A numerical investigation using in-house code is performed to encapsulate the effect of solid boundaries on two-phase laminar flow. The specific problem of plume rise is tackled using the Level Set method. The plume is considered to have negligible surface tension effects and is solely driven by density differences, such that the density ratio is fixed to two. The Navier-Stokes solver is coupled to the Level Set advection subroutine explicitly. A high-resolution WENO-5 scheme is used with the Runge Kutta (RK) 4th order multi-step method for time marching of the Level Set function. Re-initialization and Level Set advection are implemented using the same spatial discretization subroutine but re-initialization procedure leverages TVD RK-3 scheme for temporal discretization. The presence of walls of confinement profoundly impacts the rising plume and its breaking up in other fluid, providing non-intuitive results as the lighter fluid rises up differently from the way it would have in an unbounded case. Plume diameter is varied as fraction of cavity width for detailed understanding of underlying effects.

Keywords: Plume Rise, WENO-5, Runge-Kutta 4th order, TVD RK-3, Level Set

1. INTRODUCTION

Most of the flows that we encounter in our daily lives are multiphase flows. Be it blood flowing in our veins or clouds in the sky, all of them are examples of multiphase flows [1]. Two-phase flows are a kind of multiphase flow that comprises only two distinct phases. The terms phase and components are mostly used interchangeably despite obvious distinctions, like oil-water emulsion also falls under the category of two-phase flows despite being the same phase. In two-phase flows themselves, there is a huge spectrum of physical governing laws applicable in different conditions that vary widely from each other. For example, both sandstorms and oil-water emulsions are studied under two-phase flows, but on the one hand, where sandstorms consist of discrete sand particles transported in the air, oil-water emulsions consist of two volumes deforming within each other. They are both governed by totally different physics. Among all these categories, a class of two-phase flows is that of interfacial flows [2]. As the name suggests, interfacial flows are flows in which the interface is of prime importance. Along with all boundary conditions of fluid flow governing equations, we also require an additional boundary condition for interface evolution [3]. This kinematic boundary condition can be simulated using Level Set method introduced by Osher and Sethian [4] and have proved to be very promising candidates for such kinematic boundary condition because of their natural amalgamation with fluid flow governing differential equations, easy and efficacious implementation,

and easy extension into the third dimension. Unlike the Volume of Fluid (VOF) method, where a characteristic variable is tracked with a discretely marked value of either one or zero, Level Set works on the idea of extending the interface into one higher dimension such that the value of that higher dimensional function at any specified set level is the position of the interface, and the value of that function at any place in the domain is the signed distance from the interface. Generally, for ease of understanding, we refer to zero level set because the sign of that function itself becomes a direct indication of which fluid we are referring to. [5]. For advection of Level Set function, it is customary to use high-resolution schemes like ENO (Essentially Non-Oscillatory) and Weighted ENO to avoid area loss as much as possible [6]. Accurate advancing in time requires high-order Runge-Kutta schemes for Hamilton-Jacobi equations. There is a plethora of discussion over the existence of solutions to Hamilton-Jacobi equations, which can be found in the works of Sussman, Sethian, Osher, Shu, and many more. All of these advances vouch in the favour of Level Set methods for simulating interfacial flows. Still, area conservation is not guaranteed by whatever order scheme we implement; in fact, this is a drawback of the Level Set method. Another aspect is to make sure that the signed distance property of Level Set function does not deteriorate with time. For this, many options are available in literature like re-initialization procedure [7]. Re-initialization has a drawback, that it is extremely computational intensive. Significant algorithmic advances have been made in this direction as well, like fast marching methods by Sethian [8], which significantly improve computational requirements with an efficient sorting algorithm.

From a physical perspective, it is important to note that within the domain of interfacial flows, plumes are an interesting example that are predominantly buoyancy-driven with negligible surface tension effects at scales of interest. The mixing of plumes and studying their dynamics form an important part of studying geophysical phenomena like cloud patterns and many more. Capturing such physics is very difficult with experiments because the repeatability of experiments where multiple phases are concerned is very low [1]. The quantification of the pattern is also debatable. All of these facts tilt the discussion of two-phase flows in favor of CFD. Till the mid-1980s, it was unimaginable, but within a decade, the research progressed leaps and bounds. First was the breakthrough in schemes like ENO [9], and second was the introduction of Level Set as a tool for simulating two-phase flows [5].

2. LITERATURE REVIEW AND OBJECTIVE

In 1987, a ground-breaking work was published by Ami Harten and Stanley Osher [9] discussing a scheme that they

referred to as a uniformly high-order accurate non-oscillatory scheme. Although originally constructed for shock capture, it is today most extensively used in the approximation of hyperbolic differential equations. The idea proposed by Harten was simple but quite a bit different from the total variation minimizing schemes that already existed. Unlike TVD schemes, which level down to first-order accuracy at the most and are variation-diminishing, these schemes proposed by Harten were variation-non-increasing. The idea was to take the gradient from the direction where its magnitude was the least. In this way, the jump across the discontinuity can be avoided. Notice that for evolving fronts, this can be achieved only with a flexible stencil for gradient calculation, unlike the fixed stencil approach [10]. This was desirable since blow-up of the solution could be avoided and higher-order terms could be retained in the approximation at the same time. The problem with ENO schemes was, firstly, inefficient implementation and, secondly, abrupt changes in stencil. The first problem was tackled with min-mod limiters and vector operations; the second problem was dealt with using the weighting of different stencils and using all of them at once such that the weights adjust themselves to adapt to flow. In the same decade, the advent of the Level-Set method by Osher and Sethian(1988) [4] led to the devising of a class of ideas where an interface could be appropriately represented as an implicit surface, extending into one higher dimension. This implicit surface at a set level represents the front between two different materials, thus gaining the name Level Set. Level Set resolves the issue of singularities in solutions where merging and separation (cusps and sharp changes) happen. Interface is advanced with the whole implicit surface. The value of the implicit surface at any point is the signed distance to the interface. In the above discussion, it is clear that the function needs to be Lipschitz continuous [11]. Other methods that existed prior to the Level Set method were Volume of Fluid (VOF) and Marker and Cell (MAC). Each of them had their own challenges; for example, the VOF with geo-advection has too many if-else conditions. VOF also involves interface reconstruction step, which higher than second order is rather complex to derive and implement. MAC approach suffers from the drawback of complex interface surgery when breaking away or merging happens. This is where Level Set stands out, with only drawback being mass-conservation. LSM is purely mathematical in approach. To overcome this problem, methods like CLSVOF and Conservative Level Set method have been proposed. Regular re-initialization makes sure that the signed distance property of Level Set is maintained throughout the solution. The equation of motion of the interface resembles the Hamilton-Jacobi equation and is numerically approximated with the help of tools prepared for simulating hyperbolic equations. HJ-ENO and HJ-WENO are extremely popular due to their non-oscillatory solution properties and high-order approximation near the discontinuity. In fact, a modified equation analysis (with suitability assumptions) can simply prove that the first-order upwind (FOU) scheme for HJ equations can be stable. Although they are not used due to their extreme diffusive nature, FOU schemes could still serve as a base for extending the code into an ENO

or WENO scheme by adding few terms. If solved on a sufficiently fine grid, a F.O. upwind scheme can give us physically consistent results, for simple canonical problems. Reaping the advantages of all these advances would not have been possible without efficient implementation strategies tailored to cater to the specific needs of different problems. ENO and WENO schemes are similarly derived methods, where WENO schemes significantly improve over ENO to provide higher formal accuracy for the same stencil. Near-boundary cells can have different stencils. In fact, WENO (for problems of linear convection) schemes avoid degeneracy and other numerical problems, as discussed in detail by Rogerson and Meiburg for periodic boundary condition and the finite difference ENO scheme[12]. Shu and Rogerson and Meiburg [12] both highlight that by using multiple convex weighted fixed stencils in the ENO scheme in regions devoid of discontinuity, one can retain the formal accuracy of the claimed order.

To the best of our knowledge, near-wall effects of density-driven plumes have not yet been quantified & have been studied here, which indeed show interesting physics as we observe choking and local re-circulations along with the solid boundary effects for larger plumes, but as the diameter of the initial plume reduces, the choking reduces, and so do boundary effects. Oscillations are observed in the initial phase when choking is predominant, but the plume sooner or later becomes a thin trail as it moves up resulting in a change in scales as solution progresses.

3. NUMERICAL METHODOLOGY

In the recipe of our in-house numerical solver for two phase flows, there are three major ingredients. First and foremost is the Navier-Stokes solver for fluid flow, which has been implemented on a collocated grid with a first-order convective scheme and first-order implicit Euler temporal discretization using the SIMPLE algorithm for pressure velocity coupling in a finite volume formulation. Keeping first-order spatial discretization helps us kill many numerical instabilities. Although implicit Euler is not considered a worthy candidate for accurate time tracking, but its ease of implementation is very lucrative. Second comes Level-Set advection using a linear partial differential equation, which resembles HJ. Converged velocities from the SIMPLE loop are used to advect the Level Set with WENO-5 spatial approximation as implemented by Jiang and Peng [11] and the RK-4 multistep scheme for time marching. The impact of RK-4 on the speed of execution of computer program was very large, and we look forward to improving on that, but for now our discussion is limited to the conventional RK-4 scheme only. Third comes the re-initialization procedure, in raw form as first proposed (Sussman et al.[7]). Same subroutine that cater to LS advectors are used for the re-initialization procedure for spatial discretization with TVD RK-3 scheme for time marching. Here, Godunov schemes for flux evaluation are employed in gradients. We implemented our code in dimensional formulation instead of non-dimensional with one fluid approach, which could be established by using regularisation (Heaviside and Dirac Delta). The subscript Δ indicates regularization of the variable. In

two dimensions the continuity and momentum equations for both non-miscible fluids in incompressible flow is given as:

$$\begin{aligned} \partial_x u + \partial_y v &= 0 & (1) \\ \rho_\Delta (\partial_t u + \partial_x(uu) + \partial_y(vu)) &= -\partial_x p \\ &+ \mu_\Delta (\partial_x^2 u + \partial_y^2 u) \\ &+ \rho_\Delta \vec{g} \cdot \hat{i} & (2) \\ \rho_\Delta (\partial_t v + \partial_x(vu) + \partial_y(vv)) &= -\partial_y p \\ &+ \mu_\Delta (\partial_x^2 v + \partial_y^2 v) \\ &+ \rho_\Delta \vec{g} \cdot \hat{j} & (3) \end{aligned}$$

where,

$$\partial_x^n \phi \equiv \frac{\partial^n \phi}{\partial x^n} \quad (4)$$

$$\kappa_\Delta = \kappa_1 + (\kappa_2 - \kappa_1)H(\psi) \quad (5)$$

$$\vec{g} = -9.81 \hat{j} \frac{m}{sec^2} \quad (6)$$

In the above mentioned equations, κ is any fluid property and ψ is the Level Set function defined in entire domain and it evolves according to a linear advection equation which resembles HJ as discussed above. Which is as follows:

$$\partial_t \psi + u \partial_x \psi + v \partial_y \psi = 0 \quad (7)$$

$$||\psi|| = \frac{1}{F} \quad (8)$$

where F ($=1$, here) is the front propagation speed. In our formulation it does not matter if u and v velocities are taken outside or inside partial differential operator because the velocities are predetermined from the outer NS loop and are considered converged velocities at that time level when Level Set function is advected. Equation 8 is the condition that LS function must follow at all time levels to keep its signed distance property intact, which is implemented in form of a unsteady PDE in pseudo time and solved till steady state iteratively:

$$\partial_t \psi + S(\psi_0)(||\nabla \psi|| - 1) = 0 \quad (9)$$

$$S(\psi_0) = \frac{\psi_0}{\sqrt{\psi_0^2 + 2dx^2}} \quad (10)$$

$$\nabla \psi = \partial_x \psi + \partial_y \psi \quad (11)$$

where $S(\psi)$ corresponds to smoothed out sign of ψ over $\sqrt{2}dx$ where dx is the cell width in uniform mesh. $||\psi||$ refer to Eulerian distance from front. Finally, it is highlighted that Godunov flux definition is directly absorbed from Jiang and Peng [11] and is approximated using same WENO-5 formulation on a uniform mesh for gradient calculations. Details of implementation of re-initialization procedure are skipped for brevity.

3.1. Validation

Three validations in total have been performed to determine if the numerical solver developed is capable of capturing correct physical phenomena or not, which are as follows:

- 1) Lid-driven cavity as proposed by Ghia et al. (1982) [13] for fluid flow solver loop. Y vs U and V vs X are plotted in Figure 2 for detailed investigation

of Co-located grid FVM flow solver. Please note that validation has not been performed for Reynolds number greater than 5000 for two reasons. Firstly, our result cases include Reynold's number of the order 10^3 and less. Secondly, First order upwind scheme on collocated formulation did not converge at Re higher than 5000. Here, we took L2 norm of mass residual as criteria for loop breaker, numerically equal to 10^{-6} .

- 2) Reversed Vortex in a Box test for Level Set advection was performed with initial conditions as provided by Rider and Kothe [14]. Quantification of error was performed on the lines of [15]. Here we have taken L2 norm of error for quantification (refer 1), but it can be easily proven that any L_p norm $p \in [1, \infty)$ will be minimized using our code because of Norm Equivalence theorem which says that all the norms remain within constant factor of each other. For our case, $T_{max} = 6.0 \text{ sec}$ at $Co = 0.1$. Here we must defend by highlighting that $Co = 0.1$ was intentionally chosen even though our LS advection subroutine attains neutral stability at $Co = 0.5$, this is because the results cases had a time step size restriction imposed over them due to NS loop and thus quantification of error with that time step size makes much more sense.
- 3) Rayleigh Taylor instability for testing the correct coupling of the above two subroutines. (Ref. Figure 3 with legend Yellow \equiv lighter fluid ($\rho = 1.0 \frac{Kg}{m^3}$) and Blue \equiv heavier fluid ($\rho = 2.0 \frac{Kg}{m^3}$). Details are omitted for sake of brevity.

In all the cases results match well with the results published in the literature.

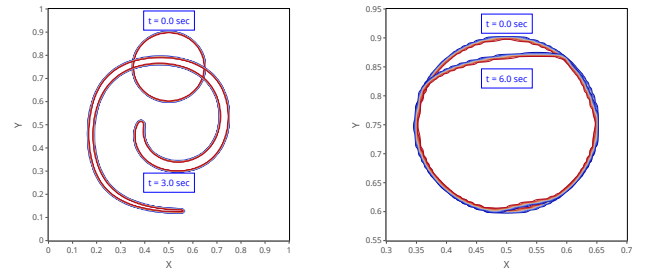


Figure 1: Reversed Vortex in a Box test with initial conditions as proposed by Rider and Kothe

4. RESULTS AND DISCUSSION

Here we discuss our findings and observations for three cases where plume diameter (D) to confinement width (L_x) ratio is varied such that D/L_x is numerically 0.98, 0.8 & 0.4, with initialization of circular patch done at same center (0.005m, 0.005m) in a rectangular flask with closed lid of width 0.01m and height to width ratio of 4 with uniform mesh of 200×800 . Evolution of solution till 0.2 sec is performed, which is long enough for observing the time scales of our interest.

Table 1: Tabulated results of L2 norm of Area mismatch for $t \in [0, T_{max}]$

S.N	N_x	Area					$ H(\psi_0) - H(\psi_f) _{L2}$
		t = 0.0	t = 3.0	ΔV (%)	t = 6.0	ΔV (%)	Area mismatch (L2)
1	100	0.07077	0.05885	-16.8443	0.0463	-34.4614	14.3888
2	120	0.07074	0.06208	-12.2444	0.0561	-20.5753	13.2630
3	150	0.07072	0.06458	-8.6824	0.0600	-15.0396	14.0803
4	170	0.07071	0.06593	-6.7686	0.0623	-11.8724	14.0582
5	200	0.07070	0.06722	-4.9203	0.0647	-8.4364	13.9266

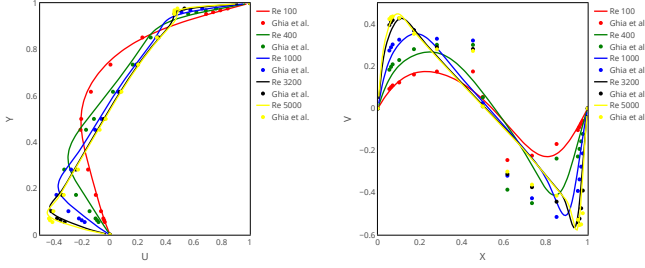


Figure 2: Lid-Driven Cavity validation

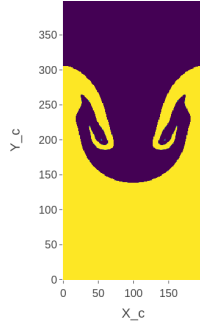


Figure 3: Rayleigh-Taylor instability at $t = 0.285$ sec. Contours lie between $1.0 \frac{Kg}{m^3}$ to $2.0 \frac{Kg}{m^3}$ with a step 0.1

For every plot given in this manuscript, corresponding time stamps (t in sec) and area loss (ΔV in %) are explicitly mentioned at the top of that particular figure. A detailed sample depicting the position of all post processed data for this section is provided as an initialization figure 4. Due to inherent area loss associated with Level Set method, the simulation is stopped once the % area loss exceeds 2% . Density ratio is fixed to 2 (refer Figure 5, 6 and 7, where Pink \equiv heavier fluid ($\rho = 2.0 \frac{Kg}{m^3}$) and Cream \equiv lighter fluid ($\rho = 1.0 \frac{Kg}{m^3}$)) and dynamic viscosity (μ) of both the fluids is considered as 10^{-5} , since it is numerically close to that of air under STP conditions. Such a case was taken since this problem could serve as testing bed for addressing particular case of thermal stratification where density ratio is close to one and Boussinesq approximation holds true. Anyway, thermal effects are not considered in this study but it is worth mentioning that Plume rising is infact a problem that is mostly found in natural setting with coupled heat

transfer effects [16], so discussing its flow physics holds prime importance from that angle. The three cases $D/L_x = 0.98, 0.8$ & 0.4 are capable of clearly capturing the following physical phenomena of our interest which are discussed in detail under subsections given below. For initialization and post process plot details refer Figure 4 and Figure 5, 6, 7.

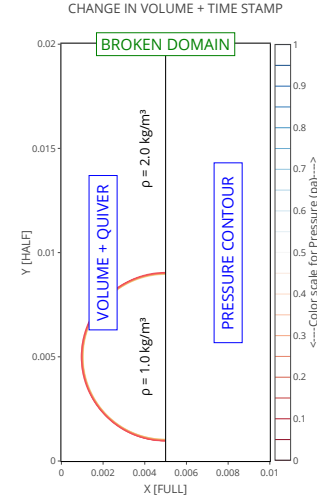


Figure 4: Initialization Plot for domain

4.1 Effect of Solid boundaries on Plume rise

As it is clearly visible from the above cases that the plume rise in a flask (with considerable D/L_x ratio) is not the same as that in unbounded conditions (results for unbounded rise are not of our interest and are not shown for the same reason). In unbounded conditions, plume rise happens only upwards and without oscillation of fluid velocities because the plume can freely expand as it rises. But when in a flask, the effect of walls are significant. First of all, the plume has to push apart the heavier fluid to rise, but the heavier fluid has nowhere to go, since the top and sides of flask are shut. Also since the heavier fluid has to fall down due to gravitational force, it pushes the plume down and only after a significant pressure rise the heavier fluid seeps down from the side, it is then that we see the plume rise. This goes on like a cycle with an presumably observable frequency. Also interestingly, the shearing effect due to presence of walls, causes the velocity at center-line to be more than that at sides. This sticking phenomena along with gradients in heavier fluid at interface, cause local re-circulation of lighter

fluid on sides of cavity and gives each plume rise case its peculiar shape. This oscillation cycle profoundly changes the velocity inside heavier fluid causing it to flip direction. This observation is clearly visible in superimposed quiver plot on the left hand side of all the figures given below along with pressure oscillations on the right hand sides of same plots, plotted at consecutive time levels. Also, the amplitude and frequency of oscillation is diameter dependent, which change with change in effective size of plume. For the sake of brevity, we restrict ourselves to only qualitative description and do not quantify the frequency and amplitude changes.

4.2. Shearing rate and Vortical structures

Shearing rate of plume in a confinement has been also observed to change magnitudes as can be observed in superimposed quiver plots. Evidently enough these rates change as plume deforms. Unlike unbounded case where the lighter fluid would always rise, the plume in a confinement shows oscillations at small time scales (roughly a hundredth of a second) presumably because of presence of solid boundaries. In the case with $D/L_x = 0.98$, choking condition is also observed which means that the fluid is entrained in the local region for a longer period, thus being an indication that the size of plume significantly impacts its rising cum shearing behaviour. For case, $D/L_x = 0.4$ the curling up of plume tail closer to wall are clear representatives of vortexes formed due to gradients in velocity. Irrespective of D/L_x ratio, the switching of velocity directions is observed in all cases. Also the frequency of oscillation of velocities as well as pressure is reduced as the choking is relieved as plume deforms in all cases. It is now imperative to mention that irrespective of plume diameter, these effects live only up to a fraction of seconds. Once the choking is relieved as plume deforms, these oscillations also die down indicating that they are implicitly coupled to shape of plume at previous time levels. Needless to say, Level Set method is inherently not suited for studying long time evolution, thus we limit our findings to small time intervals only.

5. CONCLUSIONS

From the above study, we conclude that the presence of solid boundaries significantly impacts the rising plume and also affects many other associated factors such as shearing rates, re-circulation zones, and local entrapment or choking when the diameter to channel width ratio is significant. As this ratio decreases, entrapment of fluid and changes in oscillation frequency at shorter time scales are observed. With this qualitative study we can also imply that rising plume in a confinement can churn the fluid due to presence of buoyancy driven vortexes. This can in fact augment heat transfer rates (not considered in present study) solely due to enhanced mixing. Depending upon the size of plume, the disturbance in the flask can be tailored to obtain specific rates. Detailed quantification of this study will be carried out in near future.

REFERENCES

- [1] G. Tryggvason, R. Scardovelli, and S. Zaleski, *Direct Numerical Simulations of Gas-Liquid Multiphase Flows*. Cambridge University Press, 2011.
- [2] B. Andersson, R. Andersson, L. Håkansson, M. Mortensen, R. Sudiyo, and B. van Wachem, *Computational Fluid Dynamics for Engineers*. Cambridge University Press, 2011.
- [3] S. Lee and B. Soni, "The derivation and the computation of kinematic boundary condition," *Mathematics and Computers in Simulation*, vol. 71, no. 1, pp. 62–72, 2006.
- [4] S. Osher and J. A. Sethian, "Fronts propagating with curvature-dependent speed: Algorithms based on hamilton-jacobi formulations," *Journal of Computational Physics*, vol. 79, no. 1, pp. 12–49, 1988.
- [5] S. Osher and R. Fedkiw, *The Level Set Methods and Dynamic Implicit Surfaces*, vol. 57, pp. xiv+273. 05 2004.
- [6] C.-W. Shu, *Essentially non-oscillatory and weighted essentially non-oscillatory schemes for hyperbolic conservation laws*, pp. 325–432. Berlin, Heidelberg: Springer Berlin Heidelberg, 1998.
- [7] M. Sussman, P. Smereka, and S. Osher, "A level set approach for computing solutions to incompressible two-phase flow," *Journal of Computational Physics*, vol. 114, no. 1, pp. 146–159, 1994.
- [8] J. A. Sethian, "Fast marching methods," *SIAM Review*, vol. 41, no. 2, pp. 199–235, 1999.
- [9] A. Harten, B. Engquist, S. Osher, and S. R. Chakravarthy, *Uniformly High Order Accurate Essentially Non-oscillatory Schemes, III*, pp. 218–290. Berlin, Heidelberg: Springer Berlin Heidelberg, 1997.
- [10] Y. Chang, T. Hou, B. Merriman, and S. Osher, "A level set formulation of eulerian interface capturing methods for incompressible fluid flows," *J. Comput. Phys.*, vol. 124, p. 449–464, mar 1996.
- [11] G.-S. Jiang and D. Peng, "Weighted eno schemes for hamilton-jacobi equations," *SIAM Journal on Scientific Computing*, vol. 21, no. 6, pp. 2126–2143, 2000.
- [12] A. M. Rogerson and E. Meiburg, "A numerical study of the convergence properties of eno schemes," *Journal of Scientific Computing*, vol. 5, no. 11, pp. 151–167, 1990.
- [13] U. Ghia, K. Ghia, and C. Shin, "High-re solutions for incompressible flow using the navier-stokes equations and a multigrid method," *Journal of Computational Physics*, vol. 48, no. 3, pp. 387–411, 1982.
- [14] W. J. Rider and D. B. Kothe, "Reconstructing volume tracking," *Journal of Computational Physics*, vol. 141, no. 2, pp. 112–152, 1998.
- [15] M. Sussman and E. Fatemi, "An efficient, interface-preserving level set redistancing algorithm and its application to interfacial incompressible fluid flow," *SIAM Journal on Scientific Computing*, vol. 20, no. 4, pp. 1165–1191, 1999.
- [16] J. S. Turner, *Buoyancy Effects in Fluids*. Cambridge Monographs on Mechanics, Cambridge Univer-

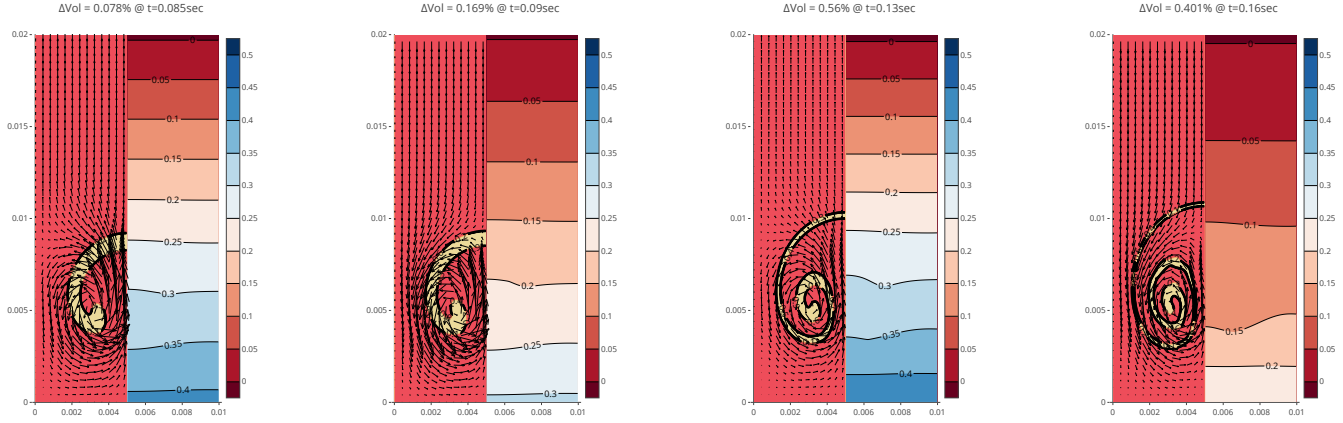


Figure 5: Plume of $D = 0.4L_x$ at $t=0.085$ sec, $t = 0.09$ sec, $t = 0.13$ sec, $t = 0.16$ sec resp.

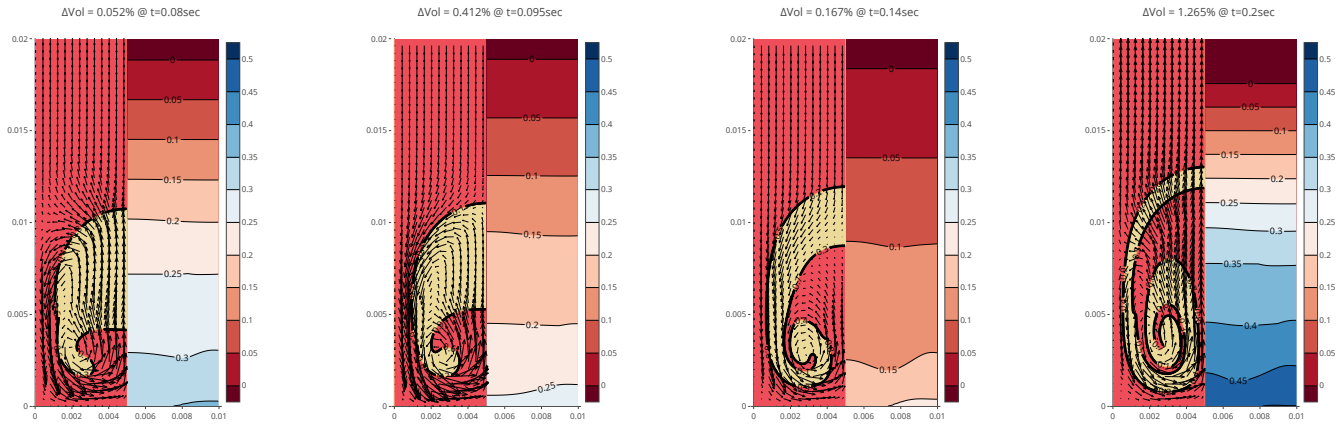


Figure 6: Plume of $D = 0.8L_x$ at $t=0.08$ sec, $t = 0.095$ sec, $t = 0.14$ sec, $t = 0.2$ sec resp.

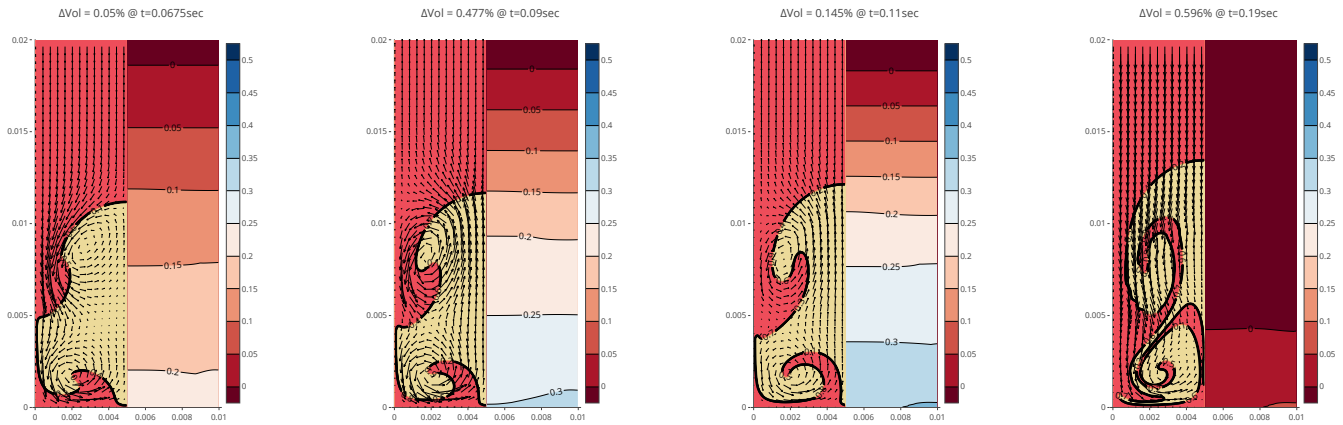


Figure 7: Plume of $D = 0.98L_x$ at $t=0.0675$ sec, $t = 0.09$ sec, $t = 0.11$ sec, $t = 0.19$ sec resp.

sity Press, 1973.